Inorg. Chem. **2007**, *46*, 3407–3418

Pyrazole Complexes as Anion Receptors: Effects of Changing the Metal, the Pyrazole Substitution Pattern, and the Number of Pyrazole Ligands

Sonia Nieto,[†] Julio Pérez,*[,†] Lucía Riera,*[,†] Víctor Riera,[†] Daniel Miguel,[‡] James A. Golen,[§] and Arnold L. Rheingold[§]

Departamento de Química Orgánica e Inorgánica-IUQOEM, Facultad de Química, Universidad de Oviedo-CSIC, 33006 Oviedo, Spain, Departamento de Química Inorgánica, Facultad de Ciencias, Universidad de Valladolid, 47005 Valladolid, Spain, and Department of Chemistry, University of California, San Diego, 9500 Gilman Drive, La Jolla, California 92093

Received January 2, 2007

Compound *cis,fac*-[Mo(η^3-allyl)(CO)$_2$(Hdmpz)$_3$]BAr′$_4$ (**1**) (Hdmpz = 3,5-dimethylpyrazole, Ar′ = 3,5-bis(trifluoromethyl)-phenyl) undergoes rapid substitution of one of the pyrazole ligands by anions, including the low nucleophilic ReO_4^-, a reaction that afforded [Mo(OReO$_3$)(η^3-allyl)(CO)$_2$(Hdmpz)$_2$] (**2**), structurally characterized by X-ray diffraction. The new compounds *fac*-[Mn(CO)$_3$(Hdmpz)$_3$]BAr′$_4$ (**4a**) and *fac*-[Mn(CO)$_3$(H^{t}Bupz)$_3$]BAr′$_4$ (**4b**) (H^{t}Bupz = 3(5)-*tert*-butylpyrazole) also undergo pyrazole substitution with most anions, and the product from the reaction with nitrate was crystallographically characterized. Compounds **4a**,**b** were found to be substitutionally stable toward perrhenate, and the adducts [Mn(CO)$_3$(Hdmpz)$_3$]·[ReO$_4$] (**7a**) and [Mn(CO)$_3$(H^{t}Bupz)$_3$]·[ReO$_4$]·[Bu$_4$N]·[BAr′$_4$] (**7b**), crystallographically characterized, display hydrogen bonds between one of the perrhenate oxygens and the N–H groups of two of the pyrazole ligands. The structurally similar adduct [Re(CO)$_3$(Hdmpz)$_3$]·[ReO$_4$] (**8**) was found to result from the interaction of [Re(CO)$_3$(Hdmpz)$_3$]BAr′$_4$ with perrhenate. The reaction of [Re(OTf)(CO)$_5$] with 3,5-dimethylpyrazole (Hdmpz) afforded [Re(CO)$_5$(Hdmpz)]OTf (**9**). The reaction of **9** with Hdmpz and NaBAr′$_4$ yielded [Re(CO)$_4$-(Hdmpz)$_2$]BAr′$_4$ (**10**), which was found to be unstable toward chloride anion. In contrast, the new compound *fac,cis*-[Re(CO)$_3$(CN^{t}Bu)(Hdmpz)$_2$]BAr′$_4$ (**11**) is stable in solution in the presence of different anions. Binding constants for **11** with chloride, bromide, and nitrate are 1–2 orders of magnitude lower than those found for these anions and rhenium tris(pyrazole) hosts, indicating that the presence of the third pyrazole ligand is crucial. Compounds *fac*-[Re(CO)$_3$(HPhpz)$_3$]BAr′$_4$ (**14**) (HPhpz = 3(5)-phenylpyrazole) and *fac*-[Re(CO)$_3$(HIndz)$_3$]BAr′$_4$ (**15**) (HIndz = indazole) are, in terms of anion binding strength and selectivity, inferior to those with dimethylpyrazole or *tert*-butylpyrazole ligands.

Introduction

Metals have been incorporated into the structures of supramolecular anion hosts for a variety of purposes.[1] Recently, it has been found that metals can serve as the major geometry-organizing element, thus allowing for a modular synthesis of the hosts, and coordination compounds with ligands featuring convergently arranged hydrogen-bond donor groups have begun to be used as anion receptors.[2]

Parkin, Reger, and Halcrow have reported the structural characterization of supramolecular adducts of the type [LnM(Hpz′)$_3$]···Cl (Hpz′ = generic pyrazole), featuring a chloride anion hydrogen-bonded by the N−H groups of three pyrazoles, the convergent geometry of which results from their bonding to the metal- or metalloid-based LnM fragment.[3] Cationic metalloreceptors [LnM(Hpz′)$_3$]$^+$ could be

* To whom correspondence should be addressed. E-mail: japm@uniovi.es (J.P.); lrm@fq.uniovi.es (L.R.). Fax: (34) 985103446 (J.P.).
† Universidad de Oviedo-CSIC.
‡ Universidad de Valladolid.
§ University of California.

(1) (a) Beer, P. D.; Gale, P. A. *Angew. Chem., Int. Ed.* **2001**, *40*, 486. (b) Steed, J. W. *Chem. Commun.* **2006**, 2637. (c) Filby, M. H.; Steed, J. W. *Coord. Chem. Rev.* **2006**, *250*, 3200.

(2) (a) Bondy, C. R.; Gale, P. A.; Loeb, S. J. *Chem. Commun.* **2001**, 729. (b) Wallace, K. J.; Daari, R.; Belcher, W. J.; Abouderbala, L. O.; Boutelle, M. G.; Steed, J. W. *J. Organomet. Chem.* **2003**, *666*, 63. (b) Bondy, C. R.; Gale, P. A.; Loeb, S. J. *J. Am. Chem. Soc.* **2004**, *126*, 5030. (c) Rice, C. R. *Coord. Chem. Rev.* **2006**, *250*, 3190.

10.1021/ic0700046 CCC: $37.00
Published on Web 03/17/2007

Scheme 1. Substitution of a Hdmpz Ligand for Chloride by Addtition of $[Bu_4N][Cl]$ to a Solution of *cis,fac*-$[Mo(\eta^3\text{-}C_3H_5)(CO)_2(Hdmpz)_3]$ (**1**)

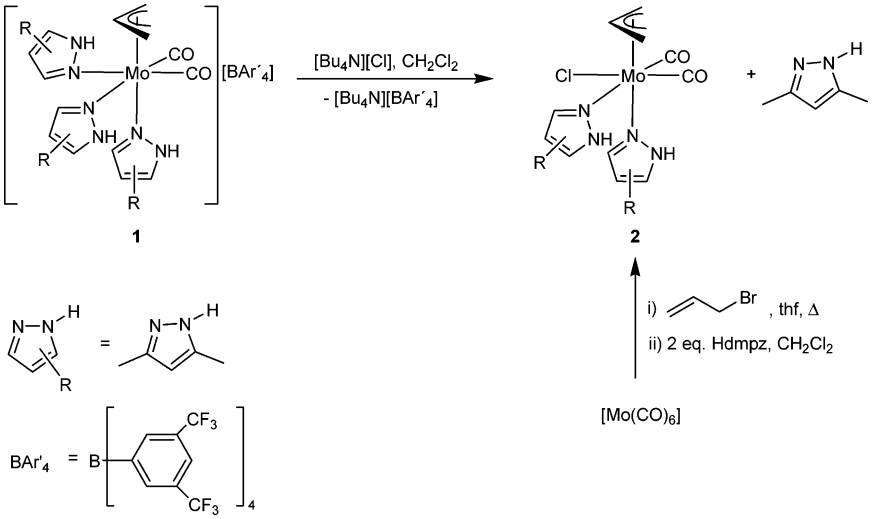

thought of as the reverse of the tris(pyrazolyl)borates and their analogues, a widely employed family of ligands.[4]

We have recently reported the synthesis of the octahedral *fac*-$[Re(CO)_3(Hpz')_3]BAr'_4$ compounds and the study of their behavior toward anions, both in solution and in the solid state.[5] These compounds constitute a new class of transition metal-based supramolecular anion receptors where the geometrical preferences of the metal are taken advantage of to organize the ditopic pyrazole molecules such that their N−H groups can converge toward an external anion. Distinctive features of our receptors are the *fac* geometry of the pyrazoles and the employment of the $BAr'_4{}^-$ (Ar′ = 3,5-bis(trifluoromethyl)phenyl) counteranion, with a high delocalization of the negative charge. In the studies carried out so far,[5] we have found that, both in solution and in the solid state (for the nitrate anion), two out of the three pyrazoles are the ones that simultaneously form hydrogen bonds with anions, and we have attributed this feature to the reluctance of our complexes to distort the L−M−L angles. We set out to complete these investigations, including structural studies of adducts with other anions as well as the behavior of other cationic octahedral *fac*-tris(pyrazole) transition metal complexes. Our results in this area are the matter of the present contribution.

Results and Discussion

Metals Other Than Rhenium. Molybdenum and Manganese Complexes. We have recently prepared the compound *cis,fac*-$[Mo(\eta^3\text{-allyl})(CO)_2(Hdmpz)_3]BAr'_4$ (**1**) (Hdmpz = 3,5-dimethylpyrazole), the structural characterization of which confirmed the *fac* disposition of the three pyrazole ligands.[6] This compound was chosen to study its behavior as an anion receptor because, in contrast to the majority of Mo(II) carbonyl complexes,[7] most pseudooctahedral molybdenum allyl dicarbonyl complexes with two coordination sites occupied by nitrogen-donor ligands are structurally rigid in solution.[8] Indeed, solution spectroscopic studies showed that the structure of the cationic complex of **1** is rigid and that no fast pyrazole exchange was taking place. In addition, complexes containing the $\{Mo(\eta^3\text{-allyl})(CO)_2\}$ fragment do not need to be handled under strictly air- and moisture-free conditions.[9]

The addition of the equimolar amount of tetrabutylammonium chloride to a CH_2Cl_2 solution of **1** led to the almost instantaneous formation of a new species with IR ν(CO) bands at 1939 and 1837 cm^{-1}, significantly lower than those found for **1** (1951 and 1863 cm^{-1}) and closely similar to those found for the neutral complex $[MoBr(\eta^3\text{-allyl})(CO)_2(Hdmpz)_2]$, recently reported by Villafañe and co-workers (1942 and 1843 cm^{-1}).[10] In fact, the new bands were found to correspond to the complex $[MoCl(\eta^3\text{-allyl})(CO)_2(Hdmpz)_2]$ (**2**), independently prepared as depicted in Scheme 1 and detailed in the Experimental Section. The ^1H NMR spectrum of the chloro complex indicates the presence of two nonequivalent pyrazole ligands, consistent with the asymmetric structure displayed in Scheme 1 and similar to the one demonstrated by X-ray diffraction for $[MoBr(\eta^3\text{-allyl})(CO)_2(Hdmpz)_2]$.[10]

Perrhenate, an anion much less nucleophilic than chloride, also effects the substitution of one of the pyrazoles in **1**. The product, complex $[Mo(OReO_3)(\eta^3\text{-allyl})(CO)_2(Hdmpz)_2]$ (**3**), was characterized by X-ray diffraction (see Figure 1). Although of poor quality, the results of the crystallographic analysis establish that its pseudooctahedral molecule consists of two Hdmpz ligands and a monodentate ReO_4^- ligand

(3) (a) Looney, A.; Parkin, G.; Rheingold, A. L. *Inorg. Chem.* **1991**, *30*, 3099. (b) Reger, D. L. Ding, Y.; Rheingold, A. L. Ostrander *Inorg. Chem.* **1994**, *33*, 4226. (c) Liu, X.; Kilner, Colin A.; Halcrow, M. A. *Chem. Commun.* **2002**, 704. (d) Renard, S. L.; Kilner, C. A.; Fisher, J.; Halcrow, M. A. *Dalton Trans.* **2002**, 4206.
(4) Trofimenko, S. *Polyhedron* **2004**, *23*, 193.
(5) (a) Nieto, S.; Pérez, J.; Riera, V.; Miguel, D.; Alvarez, C. *Chem. Commun.* **2005**, 546. (b) Nieto, S.; Pérez, J.; Riera, L.; Riera, V.; Miguel, D. *Chem.*—Eur. J. **2006**, *12*, 2244.
(6) Pérez, J.; Morales, D.; Nieto, S.; Riera, L.; Riera, V.; Miguel, D. *Dalton Trans.* **2005**, 884.
(7) Baker, P. K. *Adv. Organomet. Chem.* **1995**, *40*, 45.
(8) Pérez, J.; Riera, L.; Riera, V.; García-Granda, S.; García-Rodríguez, E. *J. Am. Chem. Soc.* **2001**, *123*, 7469.
(9) Morales, D.; Navarro Clemente, M. E.; Pérez, J.; Riera, L.; Riera, V.; Miguel, D. *Organometallics* **2002**, *21*, 4934.
(10) Paredes, P.; Miguel, D.; Villafañe, F. *Eur. J. Inorg. Chem.* **2003**, 995.

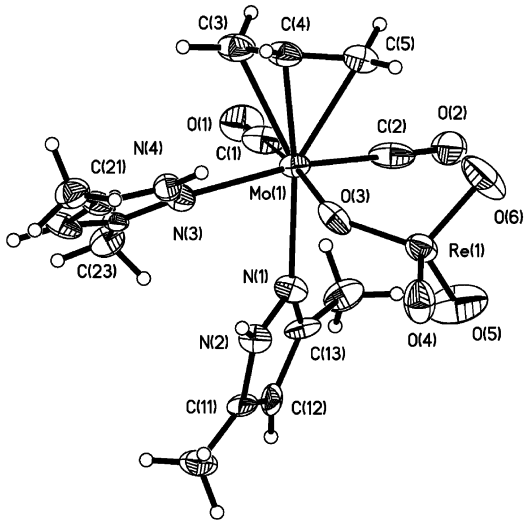

Figure 1. Thermal ellipsoid (30%) plot of *cis*,*cis*-[Mo(OReO$_3$)(η^3-allyl)(CO)$_2$(Hdmpz)$_2$] (**3**).

Scheme 2. Synthesis of the Potential New Receptors *fac*-[Mn(CO)$_3$(Hdmpz)$_3$]BAr′$_4$ (**4a**) and *fac*-[Mn(CO)$_3$(H^{t}Bupz)$_3$]BAr′$_4$ (**4b**)

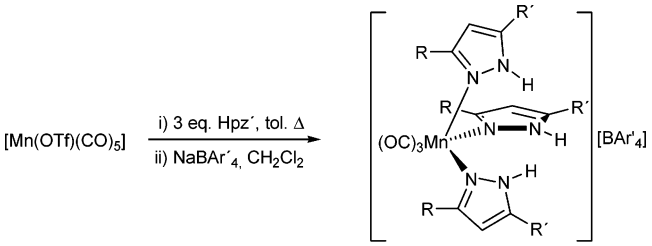

coordinated to an unremarkable *cis*-{Mo(η^3-allyl)(CO)$_2$} fragment. One of the pyrazole ligands is *trans* to the allyl group, and the other is *trans* to one of the carbonyls, so that the resulting asymmetric geometry is similar to that previously encountered for [MoBr(η^3-allyl)(CO)$_2$(Hdmpz)$_2$].[10] IR and ^{1}H NMR spectroscopies indicate that this structure is maintained in solution.

The results discussed above indicate that, due to the lability of the pyrazole ligands in compound [Mo(η^3-allyl)(CO)$_2$(Hdmpz)$_3$]BAr′$_4$ (**1**), this cannot be used as an anion receptor.

We next turned our attention to manganese compounds. The structural chemistry of Mn(I) carbonyl complexes is closely related to that of Re(I), the latter species being the ones that we initially found to be stable anion receptors.[5] Compounds *fac*-[Mn(CO)$_3$(Hdmpz)$_3$]BAr′$_4$ (**4a**) and *fac*-[Mn(CO)$_3$(H^{t}Bupz)$_3$]BAr′$_4$ (**4b**) could be readily synthesized by a method similar to the one previously employed for the synthesis of the rhenium analogues (see Scheme 2 and Experimental Section). These new compounds were characterized in solution by spectroscopy (see Experimental Section) and in the solid-state by X-ray diffraction (see Figure 2). Pyrazole complexes of Mn(I) carbonyl fragments are rare, and in only a few examples X-ray structural data are available.[11]

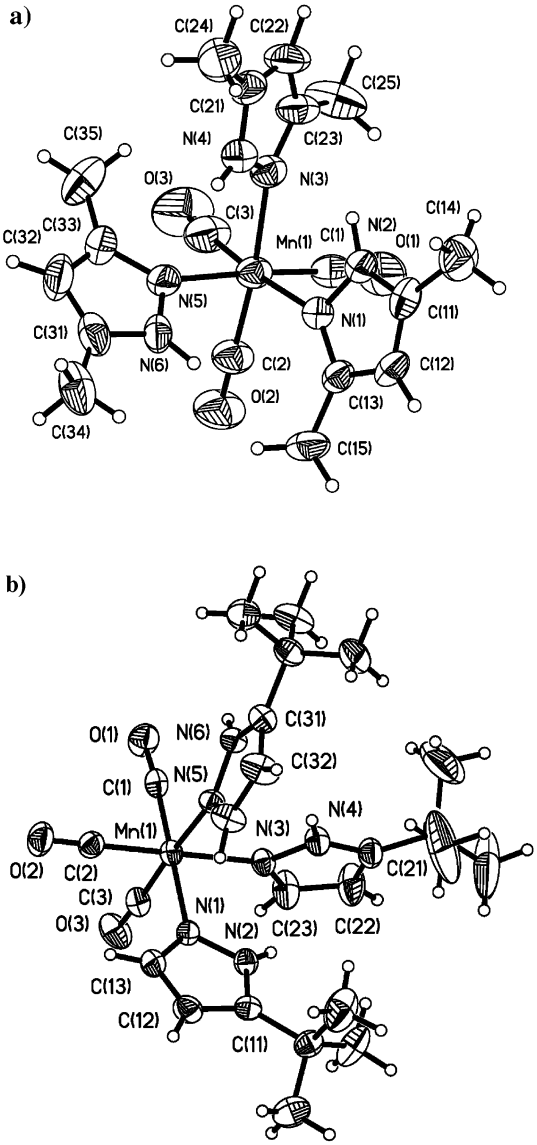

Figure 2. (a) Thermal ellipsoid (30%) plot of *fac*-[Mn(CO)$_3$(Hdmpz)$_3$]-BAr′$_4$ (**4a**). (b) Thermal ellipsoid (30%) plot of *fac*-[Mn(CO)$_3$(H^{t}Bupz)$_3$]-BAr′$_4$ (**4b**).

As expected, like their rhenium congeners, the new cationic complexes present in **4a**,**b** have pseudooctahedral geometry and a *fac* disposition of the three pyrazole ligands, both in solution (as indicated by the *fac*-tricarbonyl pattern of the ν(CO) bands in the IR spectra and by the presence of a single set of pyrazole signals in the ^{1}H NMR spectra) and in the solid state.

The reactions of **4a**,**b** with the equimolar amount of tetrabutylammonium chloride in dichloromethane afforded the products of the substitution of one of the pyrazole ligands by chloride, namely, the neutral compounds *fac*-[MnCl(CO)$_3$-(Hdmpz)$_2$] (**5a**) and *fac*-[MnCl(CO)$_3$(H^{t}Bupz)$_2$] (**5b**) (see Scheme 3 and Experimental Section). These compounds are closely similar to the manganese complexes recently reported by Villafañe and co-workers.[11] Most of the less nucleophilic anions also led to pyrazole displacement, as judged by the

(11) Arroyo, M.; Lopez-Sanvicente, A.; Miguel, D.; Villafañe, F. *Eur. J. Inorg. Chem.* **2005**, 4430.

Scheme 3. Synthesis of *fac*-[MnCl(CO)$_3$(Hpz′)$_2$] (**5a**,**b**) Complexes: Straightforward or by Substitution of an Pyrazole Ligand for Chloride Anion

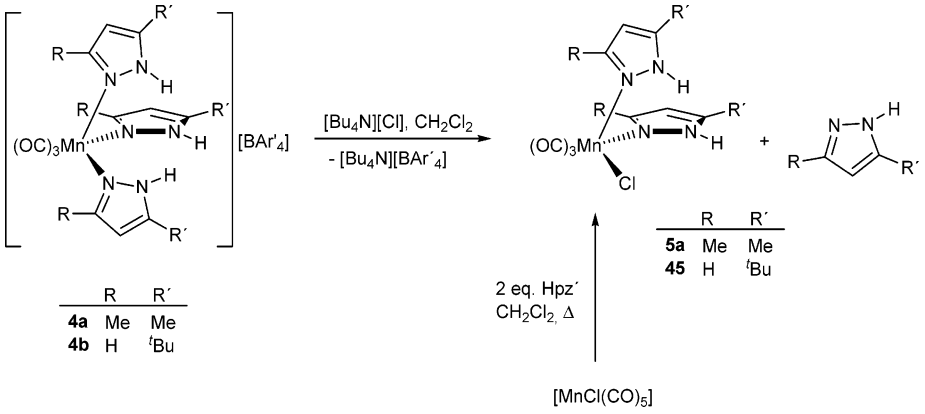

shift to significantly lower wavenumber values, typical of neutral *fac*-[MnX(CO)$_3$(Hdmpz)$_2$] complexes, in the IR ν(CO) bands. In particular, this was conclusively demonstrated for the nitrate anion. Thus, the product of the reaction of **4a** with tetrabutylammonium nitrate was isolated and its structure was determined by X-ray diffraction. The results showed that the product is an adduct in which noncoordinated 3,5-dimethylpyrazole (resulting from its displacement by the nitrate anion out of the first metal coordination sphere) interacts only through hydrogen bonds with the new complex *fac*,*cis*-[Mn(ONO$_2$)(CO)$_3$(Hdmpz)$_2$] (**6**), featuring a monodentate nitrato ligand (see Figure 3).

The main hydrogen bond interactions in the [**6**]·[Hdmpz] adduct are shown as dotted lines in Figure 3. The N−H group of the second-sphere pyrazole acts as hydrogen bond donor toward two of the oxygen atoms of the nitrato ligand (O(5)···N(8) = 3.283(4) Å, H(8)···O(5) = 2.427 Å, N(8)···H(8)···O(5) = 174.9(3)°; O(4)···N(8) = 3.270(4) Å, H(8)···O(4) = 2.695 Å, N(8)···H(8)···O(4) = 125.6(3)°), and its pyridine-type nitrogen acts as hydrogen bond acceptor toward the N−H group of one of the pyrazole ligands (N(2)···N(7) = 2.904(4) Å, H(2)···N(7) = 1.947 Å, N(2)···H(2)···N(7) = 163.3(3)°). In addition, there is an interligand nitrato−pyrazole hydrogen bond (N(4)···O(4) = 2.871(4) Å, H(4)···O(4) = 2.515 Å; N(4)···H(4)···O(4) = 107.6(2)°).

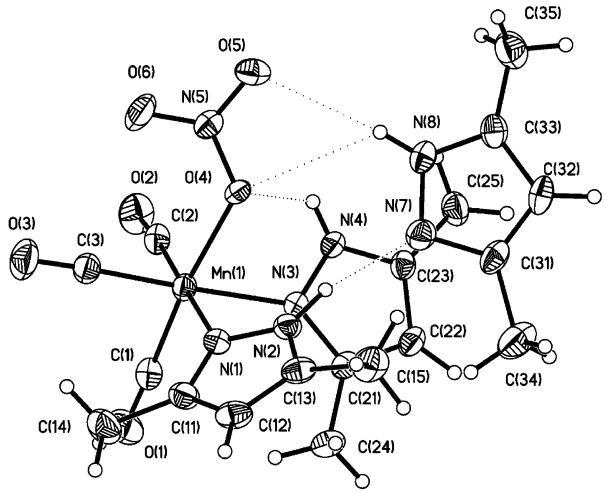

Figure 3. Thermal ellipsoid (30%) plot of the adduct *fac*,*cis*-[Mn(ONO$_2$)(CO)$_3$(Hdmpz)$_2$] (**6**) with Hdmpz. Selected distances (Å) and angles (deg) for **6**: O(5)···N(8) 3.283(4), H(8)···O(5) 2.427; N(8)···H(8)···O(5) 174.9(3), O(4)···N(8) 3.270(4), H(8)···O(4) 2.695, N(8)···H(8)···O(4) 125.6(3), N(2)···N(7) 2.904(4), H(2)···N(7) 1.947, N(2)···H(2)···N(7) 163.3(3), N(4)···O(4) 2.871(4), H(4)···O(4) 2.515, N(4)···H(4)···O(4) 107.6(2).

Unlike the molybdenum compound **1**, the manganese compounds **4a**,**b** are stable in solution (i.e., do not undergo pyrazole substitution) in the presence of the poorly nucleophilic perrhenate anion, and the 1:1 binding constants in acetonitrile were found to be 28(1) and 22(1) M^{-1}, respectively. Slow diffusion of hexane into a dichloromethane solution of an equimolar mixture of compound **4a** and [Bu$_4$N][ReO$_4$] afforded two different types of crystals, and their ^{1}H NMR spectra showed them to have the *fac*-[Mn(CO)$_3$(Hdmpz)$_3$]·[ReO$_4$] (**7a**) and [Bu$_4$N][BAr′$_4$] compositions. Such a segregation into two different phases has been previously found by us when using cationic receptors containing the BAr′$_4^-$ counteranion together with tetrabutylammonium salts. However, a similar crystallization of an equimolar mixture of compound **4b** and the salt [Bu$_4$N][ReO$_4$] yielded crystals of a single phase **7b** (see below) containing the four ions [Mn(CO)$_3$(H^{t}Bupz)$_3$]$^+$, [ReO$_4$]$^-$, [Bu$_4$N]$^+$, and [BAr′$_4$]$^-$. Thus, changes that, at first sight, one could expect to be of little significance in the exact composition of the complexes exert a dramatic effect on the composition of the crystalline phase. This is further illustrated by the fact that the nitrate adduct of the complex *fac*-[Re(CO)$_3$(H^{t}Bupz)$_3$]$^+$, the rhenium analogue of the cation present in **4b**, was found to crystallize separately from [Bu$_4$N][BAr′$_4$].[5b]

The structures of compounds **7a**,**b** were determined by single-crystal X-ray diffraction, and the results are displayed in Figure 4. For comparison purposes, the structure of the rhenium adduct [Re(CO)$_3$(Hdmpz)$_3$]·[ReO$_4$] (**8**), which crystallized separately from the salt [Bu$_4$N]·[BAr′$_4$], was also determined, and the results are displayed in Figure 5.

Two features are common to the three structures (**7a**,**b** and **8**) and to that of *fac*-[Re(CO)$_3$(H^{t}Bupz)$_3$]·[NO$_3$], mentioned above and previously determined by us:[5b] (a) only two out of the three pyrazole ligands of each cationic complex are simultaneously forming hydrogen bonds with a given oxoanion; (b) in these hydrogen bonds a single oxygen atom of the oxoanion is acting as acceptor. Additional hydrogen bonding between the third pyrazole ligand and other oxygen atoms of the oxoanion contribute to the solid-

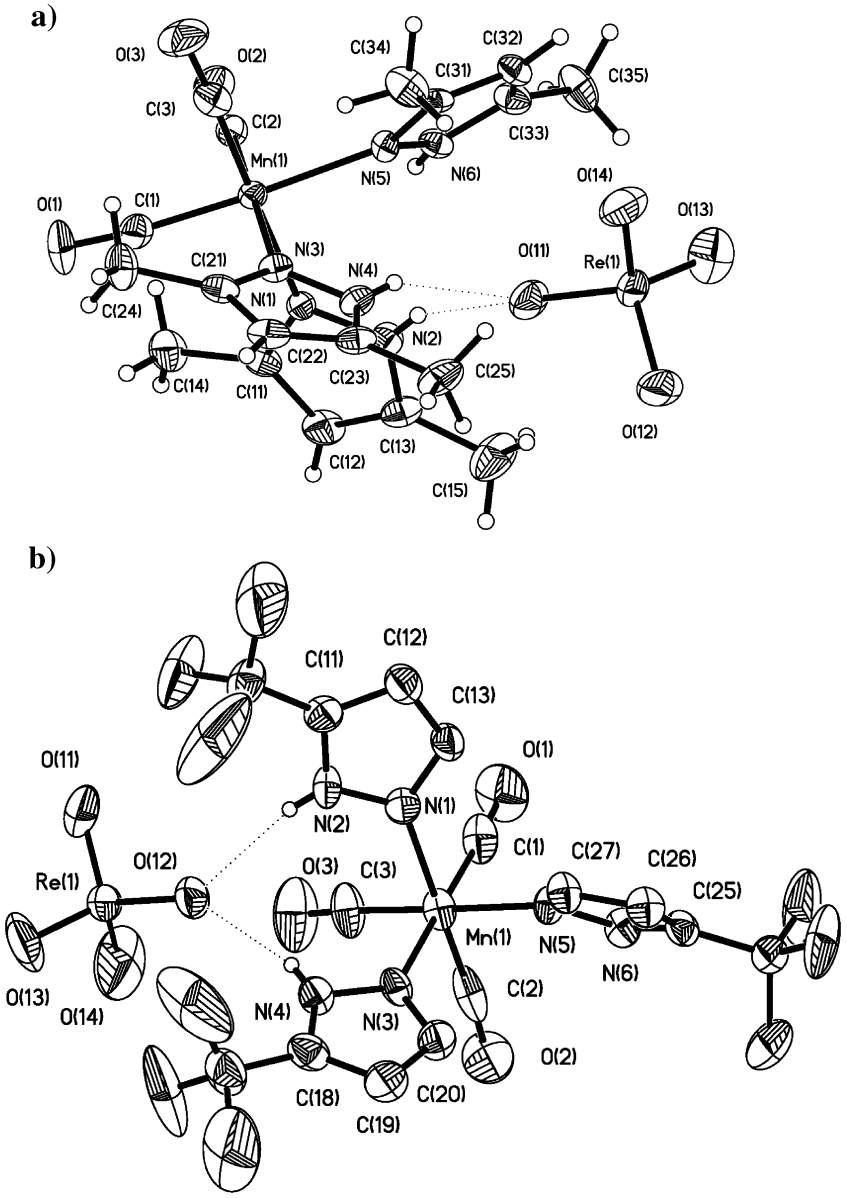

Figure 4. (a) Thermal ellipsoid (30%) plot of the adduct $[Mn(CO)_3(Hdmpz)_3]\cdot[ReO_4]$ (**7a**). (b) Thermal ellipsoid (30%) plot of the $[Mn(CO)_3(H^tBupz)_3]\cdot[ReO_4]$ adduct present in **7b**.

state network. Since these facts occur with cationic complexes containing either Mn (**7a**,**b**) or (the substantially larger) Re (**8**) as a central atom, and both in the presence (**7b**) or absence (**7a** or **8**) of the $[Bu_4N][BAr'_4]$ salt in the crystalline phase, it seems that they must be dictated by the geometry of the *fac*-$[M(CO)_3(Hpz')_3]$ (Hpz′ = generic pyrazole) complexes rather than by the size or by packing factors.

Compounds with Only Two Pyrazole Ligands. In our previous studies with *fac*-$[Re(CO)_3(Hdmpz)_3]BAr'_4$ and *fac*-$[Re(CO)_3(H^tBupz)_3]BAr'_4$ receptors, we have shown that, both in the solid state and in solution, the anionic guest forms simultaneously hydrogen bonds with only two of the three ligated pyrazoles.[5b] This is also the solid-state arrangement found in the structures discussed above.

To complete these studies, and with the goal of evaluating the effect of the presence of a third pyrazole ligand on the strength of the host−guest interaction, we set out to prepare

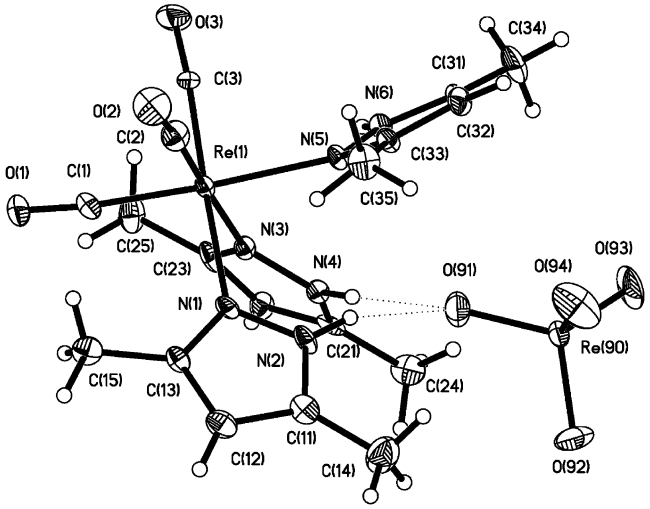

Figure 5. Thermal ellipsoid (30%) plot of the adduct $[Re(CO)_3(Hdmpz)_3]\cdot[ReO_4]$ (**8**).

Scheme 4. Synthesis of $[Re(CO)_4(Hdmpz)_2]BAr'_4$ (**10**) via the Intermediate $[Re(CO)_5(Hdmpz)]OTf$ (**9**)

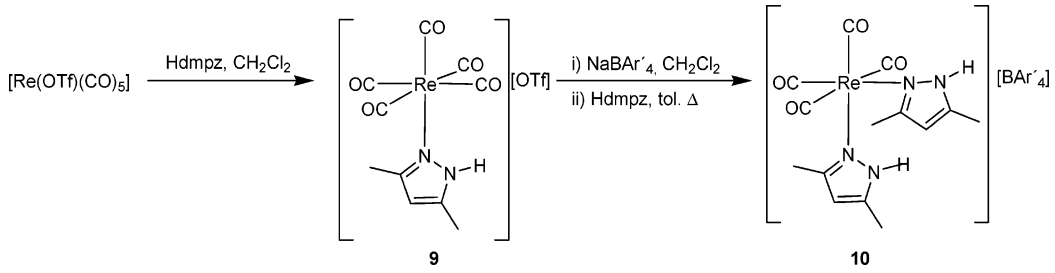

compounds of the kind *fac*,*cis*-$[Re(CO)_3(Hdmpz)_2(L)]BAr'_4$ (L = neutral, two-electron donor not able to act as a good hydrogen bond donor) and compare the strength of their anion binding with that displayed by the tris(pyrazole) compounds. We first attempted to synthesize the compound $[Re(CO)_3(Hdmpz)_2(tmpz)]BAr'_4$ (tmpz = 1,3,5-trimethylpyrazole), since the tmpz ligand would most closely mimic the electronic and steric profile of 3,5-dimethylpyrazole, while lacking its capability of engaging in strong hydrogen bonds. However, we could not find a synthetic pathway that would cleanly afford this compound. Similarly, attempts to prepare the $[Re(CO)_3(Hdmpz)_2(L)]BAr'_4$ (L = *N*-methylimidazole) led only to mixtures that could not be resolved.

On the other hand, we could successfully prepare the compound *cis*-$[Re(CO)_4(Hdmpz)_2]BAr'_4$ (**10**) as shown in Scheme 4. Compound **10** as well as the synthetic intermediate $[Re(CO)_5(Hdmpz)]OTf$ (**9**), both new compounds, were characterized by IR, ^1H NMR, and single-crystal X-ray diffraction. Thermal ellipsoid representations and selected distances and angles for compounds **9** and **10** are given in Figure 6.

The preparation and spectroscopic characterization of the pentacarbonyl pyrazole compound $[Re(CO)_5(Hpz)]BF_4$, closely related to **9**, has been previously reported by Beck and coworkers.[12]

In the solid-state structure of **9**, a hydrogen bond between the pyrazole ligand and the triflate anion is characterized by a N(2)···O(11) = 2.773(7) Å distance and a N(2)···H···O(11) = 169(5)° angle, values that suggest a relatively strong interaction. Treatment of **9** with the equimolar amount of the salt $NaBAr'_4$ in dichloromethane for a few minutes at room temperature, followed by reaction with 3,5-dimethylpyrazole in refluxing toluene, yielded *cis*-$[Re(CO)_4(Hdmpz)_2]BAr'_4$ (**10**) (see Scheme 4 and Experimental Section). However, the reaction is not clean, and **10** was obtained contaminated with a second metal−carbonyl species, as shown by the IR monitoring of the reaction. Fractional crystallization afforded pure **10**, although in a low yield.

Preliminary experiments revealed that **10** is not stable toward chloride anion in solution; thus, further study of its behavior was not pursued. Likewise, the compound $[Re(CO)_3(Hdmpz)_2(py)]BAr'_4$ (py = pyridine) turned out to be unstable toward substitution of the pyridine ligand by anions.

Fortunately, the compound *fac*,*cis*-$[Re(CO)_3(CN^tBu)(Hdmpz)_2]BAr'_4$ (**11**), prepared as summarized in Scheme 5, was found to be stable toward anions in solution (see below).

Besides its spectroscopic characterization in solution, the solid-state structure of **11** was determined by means of X-ray diffraction. The results are displayed in Figure 7.

The solution spectral data for compound **11** are consistent with a structure in solution similar to that found in the solid

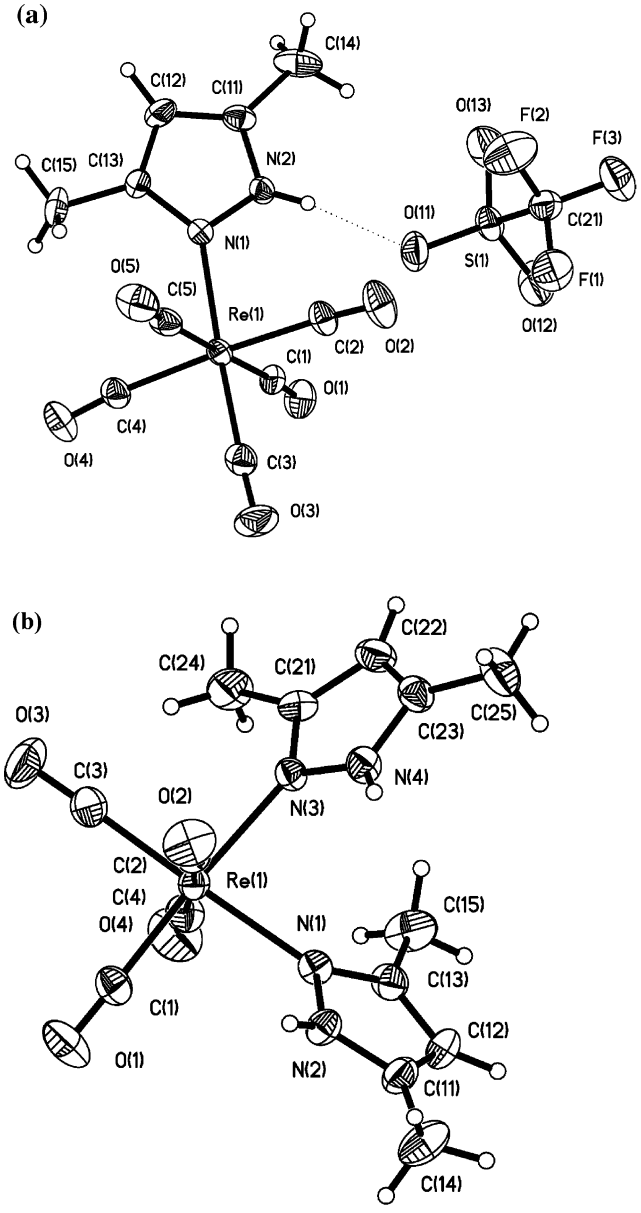

Figure 6. (a) Molecular structure of complex $[Re(CO)_5(Hdmpz)]OTf$ (**9**). Selected distances (Å) and angles (deg) for **9**: N(2)···O(11) 2.773(7); N(2)···H···O(11) 169(5). (b) Molecular structure of the cation of *cis*-$[Re(CO)_4(Hdmpz)_2]$ BAr'_4 (**10**).

(12) Appel, M.; Sacher, W.; Beck, W. *J. Organomet. Chem.* **1987**, *333*, 237.

Scheme 5. Synthesis of Compound *fac*-[Re(CN^{t}Bu)(CO)$_3$(Hdmpz)$_2$]BAr′$_4$ (**11**)

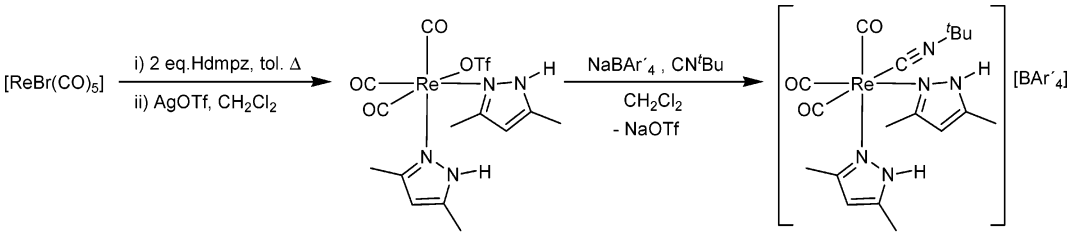

11

state. Thus, the IR spectrum in dichloromethane featured intense ν(CO) bands at 2038, 1960, and 1940 cm^{-1}, diagnostic of the *fac*-{Re(CO)$_3$} fragment, and a medium intensity ν(CN) band at 2186 cm^{-1}, due to the isocyanide ligand. As in the tris(pyrazole) complexes discussed above, the presence of separate signals for the methyl groups in the 3 and 5 positions of the pyrazole ring indicates that the pyrazole ligands are not labile.[5a] The presence of a mirror plane in the molecule of **11** is reflected in the presence of only one set of pyrazole signals in the ^{1}H NMR and ^{13}C NMR spectra and of two weak, low-field signals of different intensity, due to the two types of carbonyl ligands, in the ^{13}C NMR.

In the solid-state structure of **11**, the Re−C(isocyanide) distance, 2.078(7) Å, is only slightly longer than the Re−C(carbonyl) distances (1.926(9), 1.962(8), and 1.968(8) Å), reflecting that the isocyanide is a strong ligand, with electronic properties similar to those of carbon monoxide. The rigidity and linearity of the isocyanide ligand (Re−C(4)−N(5) = 176.8(6)° and C(4)−N(5)−C(41) = 177.1(7)°) keeps the bulky *tert*-butyl group far from the metal and from the N−H groups of the pyrazole ligands, so that its presence should not hinder the approach of the anionic guests.

Compound **11** was found to be substitutionally stable in the presence of excess of tetrabutylammonium chloride, bromide, and nitrate. Thus, in the IR spectra of such solutions, the ν(CN) band of free *tert*-butyl isocyanide at 2140 cm^{-1} could not be observed, and the wavenumber

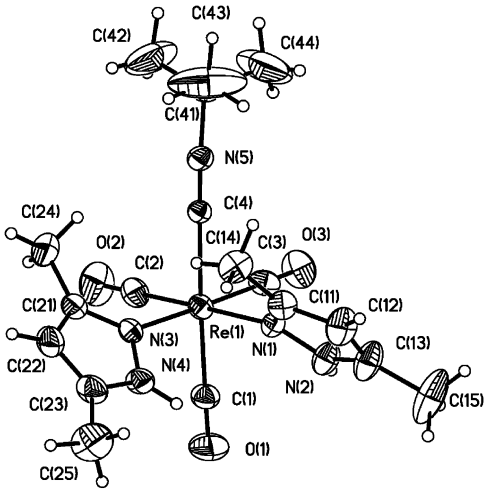

Figure 7. Thermal ellipsoid (30%) plot of the cation [Re(CN^{t}Bu)(CO)$_3$(Hdmpz)$_2$]$^+$ of compound **11**. Selected distances (Å) and angles (deg) for **11**: Re(1)−C(4) 2.078(7); Re−C(4)−N(5) 176.8(6), C(4)−N(5)−C(41) 177.1(7).

Scheme 6. Proposed Equilibria in Solution of Compounds *fac*-[M(CO)$_3$(Hpz′)$_3$]BAr′$_4$ in the Presence of an External Anion

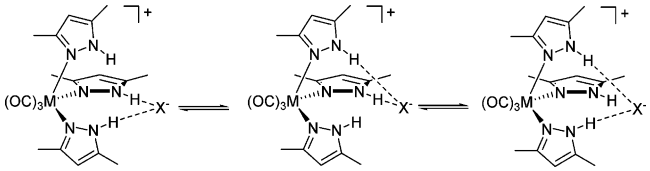

values of the ν(CO) bands corresponding to **11** undergo only relatively minor changes to lower wavenumber values attributed to the small increase in electron density resulting from the anion hydrogen bonding. Thus, for instance, the addition of 1 equiv of chloride shifts the higher frequency ν(CO) band from 2040 to 2032 cm^{-1}. This change is the largest found for all the studied anions. The ^{1}H NMR spectra of the **11**·[Bu$_4$NX] mixtures did not show evidence of free 3,5-dimethylpyrazole, and the changes were found to be dependent on the amount of anion added and to be consistent with the formation of hydrogen bonds between the pyrazole N−H groups and the anion. Thus, the shift to lower field of the pyrazole N−H signals as a response to the anion addition was used to calculate the binding constants. These were found to be 75(7), 174(7), and 133(11) M^{-1} (in CD$_3$CN) for chloride, bromide, and nitrate, respectively. These values are 1−2 orders of magnitude lower that those obtained for these anions and the receptor *fac*-[Re(CO)$_3$(Hdmpz)$_3$]BAr′$_4$.[5] Therefore, in spite of the fact that the low-temperature ^{1}H NMR spectroscopy showed that the instantaneous solution structures are consistent with an interaction of the anionic guest with only two of the three ligated pyrazoles[5b] and that it is also the kind of interaction found in the solid state, the presence of a third pyrazole ligand significantly enhances the strength of the receptor−guest interaction. This cannot be explained on the basis of the different electronic properties of the pyrazole and the isocyanide as ligands. In fact, the isocyanide is a stronger acceptor than the pyrazole, and therefore, if there is any effect of the presence of either pyrazole or isocyanide as the third ligand on the N−H groups of the anion-binding pyrazoles, it should be to make stronger those hydrogen-bond donors of the isocyanide-containing complex. As mentioned above, since the bulky ^{t}Bu group is relatively away from the N−H groups, steric hindrance does not seem an attractive explanation. Rather, we speculate that the higher binding constants for the tris(pyrazole) compounds can be attributed to the presence of three equivalent host−guest interactions of sufficient strength and which interconversion should be kinetically facile (see Scheme 6). On the other hand, we do not rule out the possibility that an

additional, weaker hydrogen bond between the anion and the N−H group of the third pyrazole could account for the difference in binding constants between complexes with two or three pyrazoles.

Different Pyrazole Ligands. Since the geometry of the interaction between the anionic guest and the cationic $[M(CO)_3(Hpz')_3]$ (Hpz′ = generic pyrazole) host is qualitatively the same for the complexes of either 3,5-dimethylpyrazole or 3(5)-*tert*-butylpyrazole, we decided to investigate how the choice of different pyrazole ligands could affect the behavior of the tris(pyrazole) complexes toward anions.

Manganese and rhenium complexes of nonsubstituted pyrazole were prepared using the same simple procedure that allowed us to isolate the aforementioned derivatives of substituted pyrazole. The new compounds *fac*-$[Mn(CO)_3(Hpz)_3]BAr'_4$ (**12**) and *fac*-$[Re(CO)_3(Hpz)_3]BAr'_4$ (**13**) were spectroscopically characterized by IR and NMR. Like its dimethyl- or *tert*-butyl-substituted congeners, the manganese compound **12** was found to resist pyrazole substitution when treated with perrhenate (a 1:1 binding constant of 28(1) M^{-1} was found for this anion in acetonitrile) but to undergo pyrazole substitution in the presence of chloride, bromide, and nitrate. Compound **13** was found to be substitutionally stable toward bromide, nitrate, and perrhenate, and binding constants of 540(27), 112(13), and 63(1) M^{-1}, respectively, were calculated for these anions (CD_3CN). However, treatment of **13** with tetrabutylammonium chloride led to substitution of one of the pyrazole ligands by chloride. This result contrasts with the stability showed by the 3,5-dimethylpyrazole or the 3(5)-*tert*-butylpyrazole analogues. The difference can be explained by the steric protection lent by the substituents, previously noted when comparing the behavior of *fac*-$[Re(CO)_3(Hdmpz)_3]BAr'_4$ and *fac*-$[Re(CO)_3(H^tBupz)_3]BAr'_4$ receptors.[5b]

The presence of planar aromatic rings as substituents at the pyrazole ligands can give rise to stronger hydrogen bond donor N−H groups (due to the electron-withdrawing character of the aryl groups when compared with methyl or *tert*-butyl groups) and perhaps to a more discriminating binding cavity if the aryl groups are adequately disposed. Therefore, we set out to prepare tris(pyrazole) receptors featuring aromatic groups. Compound *fac*-$[Re(CO)_3(HPhpz)_3]BAr'_4$ (**14**) (HPhpz = 3(5)-phenylpyrazole) was prepared by the method used for the derivatives mentioned above and spectroscopically characterized (see Experimental Section). Compound **14** was found to be stable toward chloride, bromide, iodide, nitrate, hydrogensulfate, and perrhenate, and 1:1 binding constants of 2406(125), 1712(90), 80(1), 1592(1), 147(1), and 67(9) M^{-1}, respectively, were calculated for these anions in deuterated acetonitrile. Albeit comparable, these values do not offer a clear advantage when compared with the behavior of *fac*-$[Re(CO)_3(Hdmpz)_3]BAr'_4$ and *fac*-$[Re(CO)_3(H^tBupz)_3]BAr'_4$ receptors.

Indazole (HIndz) features a fused aromatic ring and thus can be regarded as a rigid phenyl-substituted pyrazole. Compound *fac*-$[Re(CO)_3(HIndz)_3]BAr'_4$ (**15**) (see Experimental Section for the synthesis and characterization) was found to be stable toward chloride, bromide, iodide, nitrate, hydrogensulfate, perrhenate, and perchlorate. Binding constants for these anions, displayed in Table 1, indicate an interaction weaker than that found for the tris(pyrazole) complexes and no selectivity. More basic anions such as fluoride and dihydrogen phosphate were found to deprotonate **15** to afford a neutral complex, as indicated by the large shift to lower wavenumber values in the IR ν(CO) bands, a behavior also displayed by the previously reported tris(pyrazole) complexes derived from Hdmpz or H^tBupz.[5b] The solid-state structures of the 1:1 adducts *fac*-$[Re(CO)_3(HIndz)_3]\cdot[ReO_4]$ (**16**) and *fac*-$[Re(CO)_3(HIndz)_3]\cdot[ClO_4]$ (**17**) were determined by X-ray diffraction, and the results are shown in Figure 8.

Table 1. Binding Constant Values for Compound **15** in CD_3CN

anions	K_a (M^{-1})	anions	K_a (M^{-1})
Cl^-	320 ± 6	HSO_4^-	141 ± 6
Br^-	404 ± 2	ReO_4^-	48 ± 6
I^-	100 ± 2	ClO_4^-	10.5 ± 0.2
NO_3^-	295 ± 2		

The most revealing feature of these structures is that, unlike in the adducts of the pyrazole compounds, now only one of the N−H bonds of each cationic complex forms a

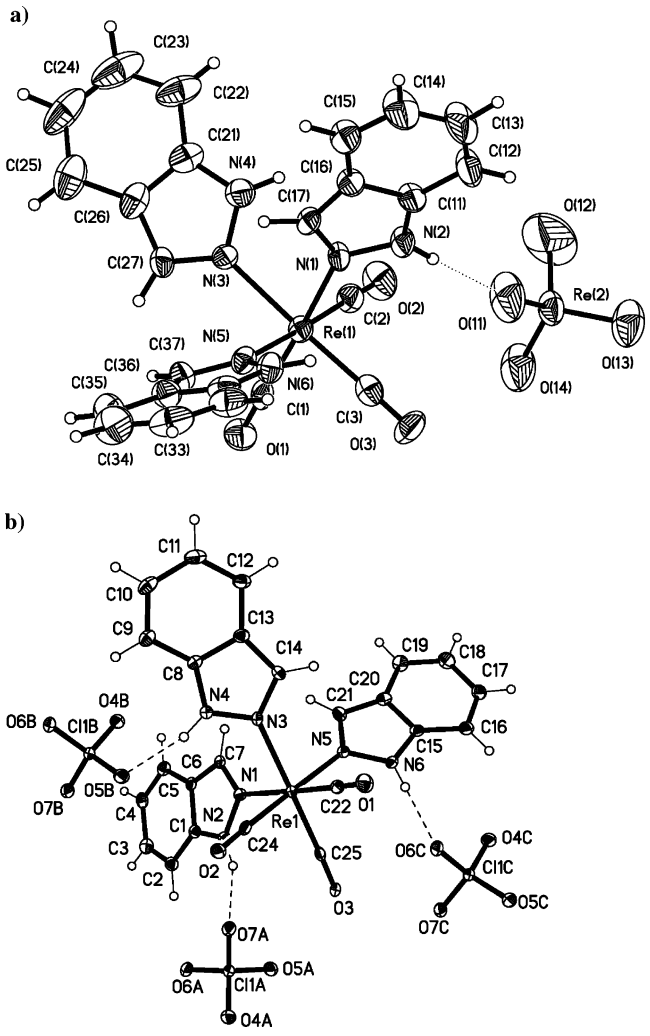

Figure 8. (a) Thermal ellipsoid (30%) plot of the adduct *fac*-$[Re(CO)_3(HIndz)_3]\cdot[ReO_4]$ (**16**). (b) Thermal ellipsoid (50%) plot of the adduct *fac*-$[Re(CO)_3(HIndz)_3]\cdot[ClO_4]$ (**17**).

hydrogen bond to a given anion. Therefore, the main effect of the fused ring, rather than providing an extra hydrogen bond donor, seems to be hindering the anion approach. As indicated by the comparison of the binding constants (that reach higher values for the tris(phenylpyrazole) derivative), this effect must be much more pronounced for the indazole derivatives, where the benzene ring is rigidly linked to the pyrazole ring, than for the phenylpyrazole derivatives, where there must be free rotation around the phenyl−pyrazole bond.

Conclusion

Unlike previously reported rhenium compounds *fac*-$[Re(CO)_3(Hpz^*)_3]BAr'_4$ (Hpz* = Hdmpz or H^{t}Bupz), molybdenum and manganese cationic tris(pyrazole) hosts *cis*,*fac*-$[Mo(\eta^3\text{-allyl})(CO)_2(Hdmpz)_3]BAr'_4$ (**1**) and *fac*-$[Mn(CO)_3(Hpz^*)_3]BAr'_4$ (Hpz* = Hdmpz (**4a**) or H^{t}Bupz (**4b**)) are labile toward most anions. The geometry of the adduct formed between the cationic complex and perrhenate (the only anion for which no pyrazole substitution at the manganese center takes place) is the same for manganese and rhenium complexes.

Although the hydrogen bonding between these tris(pyrazole) compounds and anions occurs mainly through two of the three N−H groups, the presence of the third pyrazole ligand gives rise to a large enhancement of the binding strength compared with the bis(pyrazole) compound *fac*,*cis*-$[Re(CO)_3(CN^tBu)(Hdmpz)_2]BAr'_4$ (**11**).

Taking into account the stability of the receptors, the strength of anion binding, and the difference in binding strength as a response to the nature of the anion, the rhenium receptors with 3,5-dimethylpyrazole or *tert*-butylpyrazole perform better than complexes of Mo or Mn and than Re complexes with nonsubstituted pyrazole, 3(5)-phenylpyrazole or indazole.

Experimental Section

All manipulations were carried out under a nitrogen atmosphere using Schlenk techniques. Compounds **1**,[6] $[MnCl(CO)_5]$,[13] $[MnBr(CO)_5]$,[13] and $[ReBr(CO)_5]$[14] were prepared as previously reported. Tetrabutylammonium salts were purchased from Fluka or Aldrich. Deuterated acetonitrile and dichloromethane (Cambridge Isotope Laboratories, Inc.) were stored under nitrogen in Young tubes and used without further purification. ^{1}H NMR and ^{13}C NMR spectra were recorded on a Bruker Advance 300, DPX-300, or Advance 400 spectrometer. NMR spectra are referred to the internal residual solvent peak for ^{1}H and $^{13}C\{^1H\}$ NMR. IR solution spectra were obtained in a Perkin-Elmer FT 1720-X spectrometer using 0.2 mm CaF_2 cells. NMR samples were prepared under nitrogen using Kontes manifolds purchased from Aldrich. Oven-dried 5 mm NMR tubes were subjected to several vacuum−nitrogen cycles, filled with the solution of the receptor (prepared separately in a Schlenk tube, typically in a 10^{-2} M concentration in CD_3CN) by means of a 1 mL syringe, and stoppered with rubber septa. After the NMR spectrum of the receptor was recorded, the successive aliquots of the tetrabutylammonium salt (typically 4×10^{-2} M in CD_3CN, separately prepared and kept in a septum-stoppered vial during the titration) were injected through the septum using Hamilton microsyringes (10−100 μL). The volume of each addition was 10 μL before reaching the saturation zone (nearly horizontal line of the titration profile) and 20 or 40 μL afterward. When the change in δ is small (as for ReO_4^-), 20 μL of salt solution was added from the beginning. Data were treated using the WinEQNMR program.[15]

Synthesis of $[MoCl(\eta^3\text{-}C_3H_5)(CO)_2(Hdmpz)_2]$ (2). A solution of $[Mo(CO)_6]$ (0.100 g, 0.379 mmol) in thf (20 mL) was refluxed until the IR spectrum showed the disappearance of the ν(CO) band corresponding to the starting material (1981 cm^{-1}, ca. 8 h). The resulting solution was then allowed to reach room temperature, allyl chloride (0.28 mL, 3.800 mmol) was added, and the mixture was refluxed and stirred for 15 min. The solvent was evaporated under reduced pressure to a volume of 2 mL, CH_2Cl_2 (20 mL) and Hdmpz (0.073 g, 0.380 mmol) were added, and the reaction mixture was stirred for 10 min. Then the resulting yellow solution was concentrated under vacuum to a volume of 5 mL; addition of hexane caused the precipitation of a yellow solid which was washed with hexane (2 × 20 mL). Yield: 0.135 g, 84%. IR (CH_2Cl_2): ν 1939, 1838 cm^{-1} (CO). ^{1}H NMR (CD_2Cl_2): δ 11.41 [s, br, 1H, N*H* of Hdmpz], 10.71 [s, br, 1H, N*H* of Hdmpz], 6.00 [s, 1H, C*H* of Hdmpz], 5.83 [s, 1H, C*H* of Hdmpz], 3.98 [s, 1H, H_c of η^3-C_3H_5], 3.76 [m, 1H, H_{syn} of η^3-C_3H_5], 3.09 [m, 1H, H_{syn} of η^3-C_3H_5], 2.96 [s, 3H, CH_3 of Hdmpz], 2.26 [s, 3H, CH_3 of Hdmpz], 2.15 [s, 3H, CH_3 of Hdmpz], 2.09 [s, 3H, CH_3 of Hdmpz], 1.57 [d ($^3J_{HH}$= 11 Hz), 1H, H_{anti} of η^3-C_3H_5], 1.25 [d ($^3J_{HH}$ = 11 Hz), 1H, H_{anti} of η^3-C_3H_5]. Anal. Calcd for $C_{15}H_{21}ClMoN_4O_2$: C, 42.82; H, 5.03; N, 13.32. Found: C, 42.74; H, 5.11; N, 13.29.

Synthesis of $[Mn(CO)_3(Hdmpz)_3]BAr'_4$ (4a). AgOTf (0.140 g, 0.546 mmol) was added to a solution of $[MnBr(CO)_5]$ (0.150 g, 0.546 mmol) in CH_2Cl_2 (20 mL), and the mixture was stirred in the dark for 15 min. The resulting AgBr was filtered off and the solvent evaporated under reduced pressure. The residue was redissolved in toluene (30 mL), Hdmpz (0.158 g, 1.638 mmol) was added, and the mixture was refluxed for 20 min. The yellow solution was evaporated to dryness. The residue was dissolved in CH_2Cl_2 (20 mL), $NaBAr'_4$ (0.484 g, 0.546 mmol) was added, and the mixture was stirred at room temperature for 15 min. The solution was filtered via canula, and the solvent was reduced under vacuum to a volume of 5 mL. Addition of hexane (10 mL) caused the precipitation of a yellow solid, which was washed with hexane (2 × 20 mL). Slow diffusion of hexane (15 mL) into a solution of **4a** in CH_2Cl_2 (5 mL) afforded yellow crystals, one of which was employed for an X-ray structural determination. Yield: 0.599 g, 85%. IR (CH_2Cl_2): ν 2043, 1949 cm^{-1} (CO). ^{1}H NMR (CD_2Cl_2): δ 8.82 [s, br, 3H, N*H* of Hdmpz], 7.70 [m, 8H, H_o of BAr'_4], 7.54 [m, 4H, H_p of BAr'_4], 6.24 [s, 3H, C*H* of Hdmpz], 2.43 [s, 9H, CH_3 of Hdmpz], 2.19 [s, 9H, CH_3 of Hdmpz]. $^{13}C\{^1H\}$ NMR (CD_2Cl_2): δ 219.8 [*C*O], 162.2 [q ($^1J_{CB}$ = 49.9 Hz), C^i of BAr'_4], 157.9, 145.9 [C^3 and C^5 of Hdmpz], 135.2 [C^o of BAr'_4], 129.3 [q ($^2J_{CF}$ = 33.1 Hz), C^m of BAr'_4], 125.0 [q ($^1J_{CF}$ = 271.7 Hz), *C*F$_3$ of BAr'_4], 117.9 [C^p of BAr'_4], 110.6 [C^4 of Hdmpz], 15.2 [*C*H$_3$ of Hdmpz], 11.2 [*C*H$_3$ of Hdmpz]. Anal. Calcd for $C_{50}H_{36}BF_{24}MnN_6O_3$: C, 46.53; H, 2.81; N, 6.51. Found: C, 46.68; H, 3.05; N, 6.48.

Synthesis of $[Mn(CO)_3(H^tBupz)_3]BAr'_4$ (4b). Compound **4b** was prepared as described above for **4a** from $[MnBr(CO)_5]$ (0.150 g, 0.546 mmol), AgOTf (0.140 g, 0.546 mmol), H^{t}Bupz (0.203 g, 1.638 mmol), and $NaBAr'_4$ (0.484 g, 0.546 mmol). Slow diffusion of hexane into a concentrated solution of **4b** in CH_2Cl_2 afforded

(13) Schmidt, S. P.; Trogler, W. C.; Basolo, F. *Inorg. Synth.* **1990**, *28*, 160.
(14) Reimer, K. J.; Shaver, A. *Inorg. Synth.* **1990**, *28*, 160.
(15) Hynes, M. J. *J. Chem. Soc., Dalton Trans.* **1993**, 311.

crystals, one of which was employed for an X-ray determination. Yield: 0.608 g, 81%. IR (CH_2Cl_2): ν 2048, 1956 cm^{-1} (CO). ^1H NMR (CD_2Cl_2): δ 8.92 [s, br, 3H, N*H* of H^{t}Bupz], 7.74 [m, 8H, H_o of BAr′$_4$], 7.61 [s, br, 3H, C*H* of H^{t}Bupz], 7.58 [m, 4H, H_p of BAr′$_4$], 6.48 [s, br, 3H, C*H* of H^{t}Bupz], 1.23 [s, 27H, CH_3 of H^{t}Bupz]. $^{13}C\{^1H\}$ NMR (CD_2Cl_2): δ 218.0 [*C*O], 162.1 [q ($^1J_{CB}$ = 49.8 Hz), *C*^{i} of BAr′$_4$], 159.7, 146.6 [*C*^{3} and *C*^{5} of H^{t}Bupz], 135.2 [*C*^{o} of BAr′$_4$], 129.3 [q ($^2J_{CF}$ = 30.0 Hz), *C*^{m} of BAr′$_4$], 124.9 [q ($^1J_{CF}$ = 272.6 Hz), *C*F$_3$ of BAr′$_4$], 117.8 [*C*^{p} of BAr′$_4$], 106.5 [*C*^{4} of H^{t}Bupz], 31.8 [*C*(CH$_3$)$_3$ of H^{t}Bupz], 29.7 [*C*H$_3$ of H^{t}Bupz]. Anal. Calcd for $C_{56}H_{48}BF_{24}MnN_6O_3$: C, 48.93; H, 3.52; N, 6.12. Found: C, 49.25; H, 3.35; N, 5.90.

Synthesis of [MnCl(CO)$_3$(Hdmpz)$_2$] (5a). To a solution of [MnCl(CO)$_5$] (0.060 g, 0.260 mmol) in CH_2Cl_2 (15 mL) was added Hdmpz (0.050 g, 0.520 mmol), and the reaction mixture was refluxed for 2 h. The resulting yellow solution was concentrated under vacuum to a volume of 5 mL; addition of hexane caused the precipitation of a yellow solid which was washed with hexane (2 × 20 mL). Yield: 0.089 g, 93%. IR (CH_2Cl_2): ν 2033, 1940, 1911 cm^{-1} (CO). ^1H NMR (CD_2Cl_2): δ 10.74 [s, br, 2H, N*H* of Hdmpz], 5.94 [s, br, 2H, C*H* of Hdmpz], 2.25 [s, br, 6H, 2 × C*H*$_3$ of Hdmpz]. Anal. Calcd for $C_{13}H_{16}ClMnN_4O_3$: C, 42.85; H, 4.40; N, 15.28. Found: C, 43.12; H, 4.54; N, 15.98.

Synthesis of [MnCl(CO)$_3$(H^{t}Bupz)$_2$] (5b). Compound **5b** was prepared as described above for **5a** from [MnCl(CO)$_5$] (0.060 g, 0.260 mmol) and H^{t}Bupz (0.065 g, 0. 520 mmol). Compound **5b** was obtained as a yellow powder. Yield: 0.099 g, 90%. IR (CH_2Cl_2): ν 2136, 1944, 1914 cm^{-1} (CO). ^1H NMR (CD_2Cl_2): δ 11.62 [s, br, 2H, N*H* of H^{t}Bupz], 7.60 [s, br, 2H, C*H* of H^{t}Bupz], 6.14 [s, br, 2H, C*H* of H^{t}Bupz], 1.28 [s, br, 18H, (C*H*$_3$)$_3$ of H^{t}Bupz]. Anal. Calcd for $C_{17}H_{24}ClMnN_4O_3$: C, 48.29; H, 5.72; N, 13.25. Found: C, 47.98; H, 5.89; N, 12.88.

Synthesis of [Mn(ONO$_2$)(CO)$_3$(Hdmpz)$_2$] (6). A mixture of [MnBr(CO)$_5$] (0.100 g, 0.364 mmol) and Hdmpz (0.070 g, 0.728 mmol) was refluxed in toluene (20 mL) for 30 min. The solution was evaporated to dryness, the yellow residue redissolved in CH_2Cl_2 (20 mL), $AgNO_3$ (0.062 g, 0.364 mmol) added, and the reaction mixture stirred for 45 min. The resulting solution was filtered off the white solid (AgBr) via canula and concentrated under reduced pressure to a volume of 5 mL. Slow diffusion of hexane (15 mL) at −20 °C afforded yellow crystals, one of which was employed for an X-ray analysis. Yield: 0.102 g, 71%. IR (CH_2Cl_2): ν 2040, 1947, 1923 cm^{-1} (CO). ^1H NMR (CD_2Cl_2): δ 10.49 [s, br, 2H, N*H* of Hdmpz], 5.96 [s, 2H, C*H* of Hdmpz], 2.21 [s, 6H, C*H*$_3$ of Hdmpz], 2.19 [s, 6H, C*H*$_3$ of Hdmpz]. Anal. Calcd for $C_{13}H_{16}MnN_5O_6$: C, 39.71; H, 4.10; N, 17.81. Found: C, 39.68; H, 4.04; N, 17.87.

Synthesis of [Re(CO)$_5$(Hdmpz)]OTf (9). To a solution of [Re(OTf)(CO)$_5$] (0.050 g, 0.113 mmol) in CH_2Cl_2 (20 mL) was added Hdmpz (0.011 g, 0.113 mmol), and the mixture was stirred at room temperature for 30 min. The resulting colorless solution was concentrated under reduced pressure to a volume of 5 mL. Slow diffusion of hexane (15 mL) at −20 °C afforded colorless crystals, one of which was employed for an X-ray analysis. Yield: 0.059 g, 94%. IR (CH_2Cl_2): ν 2162, 2053, 2031 cm^{-1} (CO). ^1H NMR (CD_2Cl_2): δ 13.10 [s, br, 1H, N*H* of Hdmpz], 7.26 [s, 1H, C*H* of Hdmpz], 2.40 [s, 3H, C*H*$_3$ of Hdmpz], 2.34 [s, 3H, C*H*$_3$ of Hdmpz]. Anal. Calcd for $C_{11}H_8F_3N_2O_8ReS$: C, 21.47; H, 1.44; N, 5.01. Found: C, 21.39; H, 1.51; N, 4.98.

Synthesis of [Re(CO)$_4$(Hdmpz)$_2$]BAr′$_4$ (10). To a solution of compound [Re(CO)$_5$(Hdmpz)]OTf (**9**) (0.063 g, 0.113 mmol) in CH_2Cl_2 (20 mL) was added NaBAr′$_4$ (0.100 g, 0.113 mmol), and the reaction mixture was stirred at room temperature for 15 min. The colorless solution was filtered and evaporated to dryness under reduced pressure. The residue was extracted with toluene and Hdmpz (0.011 g, 0.113 mmol) was added and refluxed for 30 min affording a mixture of a tetracarbonylic and a tricarbonylic species. The solvent was evaporated in vacuum and the white residue redissolved in CH_2Cl_2 (5 mL); slow diffusion of hexane (20 mL) at −20 °C afforded colorless crystals of the tetracarbonylic compound **10**, one of which was employed for an X-ray analysis. Yield: 0.040 g, 26%. IR (CH_2Cl_2): ν 2017, 2014, 2011, 1972 cm^{-1} (CO). ^1H NMR (CD_2Cl_2): δ 9.35 [s, br, 2H, N*H* of Hdmpz], 7.74 [m, 8H, H_o of BAr′$_4$], 7.61 [m, 4H, H_p of BAr′$_4$], 6.20 [s, 2H, C*H* of Hdmpz], 2.34 [s, 6H, C*H*$_3$ of Hdmpz], 2.21 [s, 6H, C*H*$_3$ of Hdmpz]. Anal. Calcd for $C_{46}H_{28}BF_{24}N_4O_4Re$: C, 40.81; H, 2.08; N, 4.14. Found: C, 40.78; H, 2.12; N, 4.19.

Synthesis of [Re(CN^{t}Bu)(CO)$_3$(Hdmpz)$_2$]BAr′$_4$ (11). A mixture of [ReBr(CO)$_5$] (0.100 g, 0.246 mmol) and Hdmpz (0.047 g, 0.492 mmol) in toluene (20 mL) was refluxed for 30 min affording a colorless solution that was evaporated to dryness under reduced pressure. The residue was redissolved in CH_2Cl_2 (20 mL), AgOTf (0.063 g, 0.246 mmol) was added, and the reaction mixture was allowed to stir at room temperature for 1 h. The solution was then filtered via canula, and CN^{t}Bu (0.027 mL, 0.246 mmol) was added. After 15 min of stirring at room temperature, the solution was concentrated to a volume of 10 mL and addition of hexane (20 mL) caused the precipitation of **11** as a white microcrystalline solid, which was washed with hexane (2 × 15 mL). Slow diffusion of hexane (20 mL) into a concentrated solution of compound **11** in CH_2Cl_2 at −20 °C afforded colorless crystals, one of which was employed for an X-ray analysis. Yield: 0.250 g, 72%. IR (CH_2Cl_2): ν 2186 (CN); ν 2038, 1960, 1940 cm^{-1} (CO). ^1H NMR (CD_2Cl_2): δ 9.20 [s, br, 2H, N*H* of Hdmpz], 7.73 [m, 8H, H_o of BAr′$_4$], 7.58 [m, 4H, H_p of BAr′4], 6.07 [s, 2H, C*H* of Hdmpz], 2.26 [s, 6H, C*H*$_3$ of Hdmpz], 2.16 [s, 6H, C*H*$_3$ of Hdmpz], 1.53 [s, 9H, CN^{t}Bu]. $^{13}C\{^1H\}$ NMR (CD_2Cl_2): δ 191.6 [*C*O], 191.5 [2 × *C*O], 164.1 [q ($^1J_{CB}$ = 49.7 Hz), *C*^{i} of BAr′$_4$], 158.1, 147.3, [*C*^{3} and *C*^{5} of Hdmpz], 137.2 [*C*^{o} of BAr′$_4$], 131.2 [q ($^2J_{CF}$= 31.3 Hz), *C*^{m} of BAr′$_4$], 127.0 [q ($^1J_{CF}$ = 272.3 Hz), *C*F$_3$ of BAr′$_4$], 119.9 [*C*^{p} of BAr′$_4$], 110.2 [*C*^{4} of Hdmpz], 62.2 [*C*(CH$_3$)$_3$ of CN^{t}Bu], 32.2 [*C*H$_3$ of CN^{t}Bu], 17.1 [*C*H$_3$ of Hdmpz], 13.0 [*C*H$_3$ of Hdmpz]. Anal. Calcd for $C_{50}H_{37}BF_{24}N_5O_3Re$: C, 46.63; H, 2.65; N, 4.97. Found: C, 46.81; H, 2.48; N, 5.21.

Synthesis of [Mn(CO)$_3$(Hpz)$_3$]BAr′$_4$ (12). Hpz (0.059 g, 0.872 mmol) was added to a solution of [Mn(OTf)(CO)$_5$] (0.100 g, 0.291 mmol) in toluene (20 mL), and the mixture was refluxed for 1 h. The solvent was then evaporated to dryness under reduced pressure, the residue was redissolved in CH_2Cl_2 (20 mL), NaBAr′$_4$ (0.256 g, 0.291 mmol) was added, and the reaction mixture was allowed to stir at room temperature for 15 min. The solution was filtered off (via canula) the white solid (NaOTf) and concentrated to a volume of 5 mL; addition of hexane (20 mL) caused the precipitation of **12** as a yellow solid, which was washed with hexane (2 × 15 mL). Yield: 0.281 g, 80%. IR (CH_2Cl_2): ν 2049, 1958 cm^{-1} (CO). ^1H NMR (CD_2Cl_2): δ 9.88 [s, br, 3H, N*H* of Hpz], 7.86 [d ($^3J_{HH}$ = 1.7 Hz), 3H, C*H* of Hpz], 7.72 [m, 8H, H_o of BAr′$_4$], 7.60 [s, br, 3H, C*H* of Hpz], 7.57 [m, 4H, H_p of BAr′$_4$], 6.67 [m, 3H, C*H* of Hpz]. Anal. Calcd for $C_{44}H_{24}BF_{24}MnN_6O_3$: C, 43.80; H, 2.00; N, 6.97. Found: C, 43.62; H, 2.17; N, 7.08.

Synthesis of [Re(CO)$_3$(Hpz)$_3$]BAr′$_4$ (13). Compound **13** was prepared as described above for **12** from [Re(OTf)(CO)$_5$] (0.100 g, 0.210 mmol), Hpz (0.043 g, 0.632 mmol), and NaBAr′$_4$ (0.186 g, 0.210 mmol). Compound **13** was obtained as a yellow powder. Yield: 0.228 g, 81%. IR (CH_2Cl_2): ν 2042, 1936 cm^{-1} (CO). ^1H NMR (CD_2Cl_2): δ 10.26 [s, br, 3H, N*H* of Hpz], 7.85 [m, 3H, C*H*

Table 2. Selected Crystal, Measurement, and Refinement Data for Compounds **3**, **4a,b**, **6**, **7a,b**, **8**−**11**, **16**, and **17**

param	**3**	**4a**	**4b**	**6**	**7a**	**7b**
formula	$C_{15}H_{21}MoN_4O_6Re$	$C_{50}H_{36}BF_{24}MnN_6O_3$	$C_{56}H_{48}BF_{24}MnN_6O_3$	$C_{18}H_{24}MnN_7O_6$	$C_{36}H_{48}Mn_2N_{12}O_{14}Re_2$	$C_{72}H_{84}BF_{24}MnN_7O_7Re$
fw	635.50	1290.60	1374.75	489.38	1655.14	1867.41
cryst syst	triclinic	monoclinic	triclinic	monoclinic	monoclinic	monoclinic
space group	$P\bar{1}$	$P2_1/n$	$P\bar{1}$	$P2_1/c$	$P2_1/c$	$P2_1/c$
a, Å	9.907(10)	14.775(3)	10.814(7)	11.865(3)	13.887(6)	18.566(3)
b, Å	14.555(14)	26.092(6)	15.800(7)	14.837(4)	15.524(6)	28.554(5)
c, Å	16.175(16)	15.489(3)	19.850(9)	14.004(4)	23.611(10)	18.475(3)
α, deg	79.44(2)	90	74.826(14)	90	90	90
β, deg	75.718(16)	105.468(4)	76.374(15)	110.941(5)	102.224(8)	119.043(3)
γ, deg	72.794(19)	90	83.188(146)	90	90	90
V, Å^3	2144(4)	5755(2)	3175(3)	2302.6(1 1)	4975(4)	8563(3)
Z	4	4	2	4	4	4
F(000)	1216	2592	1392	1016	2640	3768
D_{calcd}, g cm^{-3}	1.969	1.490	1.438	1.412	1.809	1.449
radiatn (*λ*, Å)	Mo Kα, 0.710 73	Mo Kα, 0.710 73	Mo Kα, 0.710 73	Mo Kα, 0.710 73	Mo Kα, 0.710 73	Mo Kα, 0.710 73
μ, mm^{-1}	6.262	0.353	0.324	0.621	5.417	1.663
cryst size, mm	0.11 × 0.15 × 0.18	0.22 × 0.23 × 0.39	0.18 × 0.35 × 0.48	0.26 × 0.22 × 0.11	0.22 × 0.25 × 0.45	0.08 × 0.20 × 0.31
temp, K	296(2)	293(2)	296(2)	293(2)	293(2)	296(2)
θ limits, deg	1.31−23.41	1.56−23.30	1.09−23.68	1.84−23.37	1.50−23.35	1.25−23.31
min/max h, k, l	−10/10, −14/16, −14/17	−16/16, −29/27, −17/15	−11/12, −17/17, −22/22	−2/13, −11/16, −15/15	−14/15, −17/17, −22/26	−20/19, −22/31, −20/19
collcd reflcns	9413	25 734	14 582	10 229	21 836	38 286
unique reflcns	5976	8295	9319	3334	7155	12 336
abs	SADABS	SADABS	SADABS	SADABS	SADABS	SADABS
params/restraints	495/0	783/0	842/0	307/0	625/0	1039/0
GOF on F^2	1.056	1.043	1.061	1.001	1.027	1.011
R_1 (on F, $I > 2\sigma(I)$)	0.0925	0.0870	0.0771	0.0405	0.0562	0.0890
wR_2 (on F^2, all data)	0.2672	0.2888	0.2442	0.1118	0.1436	0.2639
max/min Δ*ρ*, e Å^{-3}	3.874 and −5.102	0.859 and −0.450	1.073 and −0.599	0.529 and −0.300	5.434 and −1.917	1.828 and −0.709

param	**8**	**9**	**10**	**11**	**16**	**17**
formula	$C_{36}H_{48}N_{12}O_{14}Re_4$	$C_{11}H_8F_3N_2O_8ReS$	$C_{46}H_{28}BF_{24}N_4O_4Re$	$C_{50}H_{37}BF_{24}N_5O_3Re$	$C_{36}H_{42}N_6O_{10}Re_2$	$C_{24}H_{18}ClN_6O_7Re$
fw	1617.66	571.45	1353.73	1408.86	1091.16	724.09
cryst syst	monoclinic	monoclinic	triclinic	monoclinic	monoclinic	orthorhombic
space group	$P2_1/c$	$P2_1/n$	$P\bar{1}$	$P2_1/n$	$P2_1/n$	$P2_12_12_1$
a, Å	13.926(3)	9.407(5)	10.6683(17)	14.532(4)	11.790(7)	10.7796(8)
b, Å	15.559(3)	18.291(10)	12.405(2)	23.467(6)	20.368(12)	12.6297(10)
c, Å	23.677(5)	10.210(6)	19.975(3)	17.381(4)	17.485(10)	19.6399(15)
α, deg	90	90	95.593(4)	90	90	90
β, deg	102.265(4)	92.686(11)	95.245(3)	103.523(5)	93.392(12)	90
γ, deg	90	90	99.650(3)	90	90	90
V, Å^3	5013.2(19)	1754.9(17)	2578.0(7)	5763(2)	4192(4)	2673.8(4)
Z	4	4	2	4	4	4
F(000)	3040	1080	1320	2768	2120	1408
D_{calcd}, g cm^{-3}	2.143	2.163	1.744	1.624	1.729	1.799
radiatn (*λ*, Å)	Mo Kα, 0.710 73	Mo Kα, 0.710 73	Mo Kα, 0.710 73	Mo Kα, 0.710 73	Mo Kα, 0.710 73	Mo Kα, 0.710 73
μ, mm^{-1}	9.697	7.116	2.490	2.231	5.829	4.699
cryst size, mm	0.13 × 0.22 × 0.49	0.34 × 0.15 × 0.12	0.27 × 0.16 × 0.11	0.42 × 0.31 × 0.20	0.30 × 0.14 × 0.12	0.26 × 0.17 × 0.17
temp, K	293(2)	296(2)	293(2)	296(2)	296(2)	100(2)
θ limits, deg	1.50−23.28	2.23−23.28	1.03−23.28	1.48−23.26	1.54−23.35	1.92−27.54
min/max *h, k, l*	−12/15, −14/17, −26/26	−8/10, −20/19, −11/10	−11/11, −10/13, −22/16	−16/14, −26/26, −17/19	−13/12, −22/21, −18/19	−13/13, −16/16, −24/25
collcd reflcns	21 799	7596	11 378	15 378	18 667	22 887
unique reflcns	7195	2518	7263	8273	6066	1032
abs	SADABS	SADABS	SADABS	SADABS	SADABS	SADABS
params/restraints	625/0	242/0	731/0	773/0	488/0	352/0
GOF on F^2	1.044	1.053	1.030	1.011	1.000	1.061
R_1 (on F, $I > 2\sigma(I)$)	0.0591	0.0282	0.0433	0.0464	0.0326	0.0232
wR_2 (on F^2, all data)	0.1572	0.0806	0.1200	0.1267	0.0763	0.0615
max/min Δ*ρ*, e Å^{-3}	6.429 and −2.628	1.007 and −1.275	0.963 and −0.701	1.511 and −0.782	1.132 and −0.694	2.564 and −0.476

of Hpz], 7.72 [m, 8H, H$_o$ of BAr′$_4$], 7.56 [m, 4H, H$_p$ of BAr′$_4$], 7.35 [m, 3H, C*H* of Hpz], 6.60 [m, 3H, C*H* of Hpz]. ^{13}C{^{1}H} NMR (CD_2Cl_2): *δ* 193.0 [*C*O], 162.1 [q ($^1J_{CB}$ = 49.9 Hz), *C*^{i} of BAr′$_4$], 144.4, 134.0, [*C*^{3} and *C*^{5} of Hpz], 135.1 [*C*^{o} of BAr′$_4$], 129.2 [q ($^2J_{CF}$ = 31.7 Hz), *C*^{m} of BAr′$_4$], 125.0 [q ($^1J_{CF}$ = 272.5 Hz), *C*F$_3$ of BAr′$_4$], 117.8 [*C*^{p} of BAr′$_4$], 109.5 [*C*^{4} of Hpz]. Anal. Calcd for $C_{44}H_{24}BF_{24}N_6O_3Re$: C, 39.51; H, 1.81; N, 6.28. Found: C, 39.73; H, 1.89; N, 5.96.

Synthesis of [Re(CO)$_3$(HPhpz)$_3$]BAr′$_4$ (14). Compound **14** was prepared as described above for **13** from [Re(OTf)(CO)$_5$] (0.100 g, 0.210 mmol), HPhpz (0.091 g, 0.631 mmol), and NaBAr′$_4$ (0.186 g, 0.210 mmol). Yield: 0.254 g, 77%. IR (CH_2Cl_2): *ν* 2039, 1935, 1925 cm^{-1} (CO). ^{1}H NMR (CD_3CN): *δ* 11.85 [s, br, 3H, N*H* of HPhpz], 7.71 [m, 21H, BAr′$_4$ and Ph of HPhpz], 7.52 [m, 9H, Ph and C*H* of HPhpz], 6.82 [s, br, 3H, C*H* of Hpz]. ^{13}C{^{1}H} NMR (CD_3CN): *δ* 193.6 [*C*O], 162.6 [q ($^1J_{CB}$ = 49.8 Hz), *C*^{i} of BAr′$_4$],

147.3, 145.5, [C^3 and C^5 of HPhpz], 134.7 [C^o of BAr'_4], 129.1 [q ($^2J_{CF}$ = 31.8 Hz), C^m of BAr'_4], 124.5 [q ($^1J_{CF}$ = 271.7 Hz), CF_3 of BAr'_4], 130.0, 129.2, 127.1, 126.7 [Ph of HPhpz], 117.3 [C^p of BAr'_4], 105.5 [C^4 of HPhpz]. Anal. Calcd for $C_{62}H_{36}BF_{24}N_6O_3Re$: C, 47.55; H, 2.32; N, 5.37. Found: C, 47.19; H, 2.68; N, 5.51.

Synthesis of $[Re(CO)_3(HIndz)_3]BAr'_4$ (15). Compound **15** was prepared as described above for **13** from $[Re(OTf)(CO)_5]$ (0.045 g, 0.102 mmol), HIndz (0.036 g, 0.306 mmol), and $NaBAr'_4$ (0.090 g, 0.102 mmol). Yield: 0.132 g, 90%. IR (CH_2Cl_2): ν 2042, 1942 cm^{-1} (CO). ^1H NMR (CD_3CN): δ 11.91 [s, br, 3H, N*H* of HIndz], 8.06 [s, 3H, C*H* of HIndz], 7.81 [m, 3H, C*H* of HIndz], 7.72 [m, 11H, H_o of BAr'_4 and C*H* of HIndz], 7.65 [m, 3H, C*H* of HIndz], 7.63 [m, 3H, C*H* of HIndz], 7.55 [m, 4H, H_p of BAr'_4], 7.40 [m, 3H, C*H* of HIndz]. Anal. Calcd for $C_{50}H_{30}BF_{24}N_6O_3Re$: C, 45.20; H, 2.03; N, 5.65. Found: C, 45.02; H, 2.20; N, 5.51.

Crystal Structure Determination. General Description for Compounds 3, 4a,b, 6, 7a,b, 8−11, and 16. A suitable crystal was attached to a glass fiber and transferred to a Bruker AXS SMART 1000 diffractometer with graphite-monochromatized Mo Kα X-radiation and a CCD area detector. One hemisphere of the reciprocal space was collected in each case. Raw frame data were integrated with the SAINT[16] program. The structures were solved by direct methods with SHELXTL.[17] An empirical absorption correction was applied with the program SADABS.[18] All non-hydrogen atoms were refined anisotropically. Hydrogen atoms were set in calculated positions and refined as riding atoms. Drawings and other calculations were made with SHELXTL. Crystal and refinement details are collected in Table 2.

General Description for Compound 17. A crystal was mounted on a CryoLoop with Paratone-N oil[19] and cooled to 100 K. Data were collected on a Bruker SMART APEX CCD diffractometer, and the structure was solved by direct methods and refined as indicated above. The Bruker suite of programs was used for data collection, structure solution, refinement, and graphical presentation. Crystal and refinement details are shown in Table 2.

Acknowledgment. We thank the Ministerio de Ciencia y Tecnología (Grants CTQ2006-08924 and CTQ2006-07036/BQU) and European Union (ERG to L.R.) for support of this work. L.R. thanks the Ministerio de Educación y Ciencia for a Ramón y Cajal contract.

Supporting Information Available: X-ray crystallographic data for compounds **3**, **4a**,**b**, **6**, **7a**,**b**, **8**−**11**, **16**, and **17** as CIF and ^1H NMR titration profiles. This material is available free of charge via the Internet at http://pubs.acs.org.

IC0700046

(16) *SAINT+. SAXI area detector integration program*, version 6.02; Bruker AXS, Inc.: Madison, WI, 1999.
(17) Sheldrick, G. M. *SHELXTL, An integrated system for solving, refining, and displaying crystal structures from diffraction data*, version 5.1; Bruker AXS, Inc.: Madison, WI, 1998.
(18) Sheldrick, G. M. *SADABS, Empirical Absorption Correction Program*; University of Göttingen: Göttingen, Germany, 1997.
(19) Hamilton Research Laboratories.